

Research Article

# Synthesis and Characterization of TiO<sub>2</sub> Nanoparticles Doping on Cellulose as Adsorbent for Removal of Rhodamine B in Aqueous Solution

Allwar Allwar<sup>1\*</sup>, Mayla Nur Fatima<sup>1</sup>, Bayu Wiyantoko<sup>1</sup>

<sup>1</sup> Department of Chemistry, Faculty Mathematics and Natural Sciences, Islamic University of Indonesia, Yogyakarta, 55584, Indonesia

\* Correspondence: 966120101@uii.ac.id

Received: 25 January 2021; Accepted: 2 February 2021; Published: 4 February 2021

**Abstract:** Cellulose from banana fruit bunch was used as a precursor for doping titanium oxide (TiO<sub>2</sub>) in producing of TiO<sub>2</sub>/cellulose adsorbent. Cellulose was obtained by chemical impregnation using potassium hydroxide (KOH) and followed by the hydrothermal process at 250°C for 5 h. The mixtures of TiO<sub>2</sub> nanoparticles and cellulose were carried out into hydrothermal reactor under de-ionized water and ethanol and heated up to 200°C for 4 h in graphite furnace. Surface morphology analysis showed that the TiO<sub>2</sub> clearly immobilized on surface of cellulose with an increasing roughness of surface and irregular size of porosity. The development of amorphous structure to crystalline phase of TiO<sub>2</sub>/cellulose was clearly observed by the XRD. The effectiveness of TiO<sub>2</sub>/cellulose for removal of rhodamine B was investigated from different parameters of adsorption in aqueous solution. Kinetic models were well described by the pseudo-first and second-order with the best correlation coefficient (R<sup>2</sup>) attributing to the occurrence of chemisorption and physisorption mechanism.

**Keywords:** Banana fruit bunch TiO<sub>2</sub>/cellulose, Nanoparticles, Adsorption, Rhodamine B.

## Introduction

The exploration of population growth has led to an increase in modern industry. The increasing utilization of dye in the industry has become the global issues in environmental problem. The dye pollutions produced by industrial activities such as textiles, paints, printing are found in many streams of water [1]. The pollutions consist of complex aromatic structure with highly hazardous materials that can lead to destruction and even death of living things and humans [2]. Rhodamine B is one of basic dyes used in many applications in industries. Although the utilization of rhodamine B was intensively controlled, their effects on the environment are still controversial. It is because of the difficulty to determine their properties separately. Various methods have been applied to reduce the level of dye pollutions in water and recovery them for example as precipitation, electrochemical reduction and reverse osmosis. Most of them are strongly considered due to high cost process and recurring expenses, which are not appropriate for the waste treatment in the small-scale industries. The alternative method with the utilization of the adsorbents have been intensively studied and widely used for the separation and purification in the aqueous solution. There have many types of adsorbents such as activated carbon, composite, cellulose and metal oxide/cellulose that are used for the removal of dye contaminants [3]. The by-products having natural cellulose such as oil palm empty fruit bunch, banana fruit bunch, sugar cane bagasse, etc. have been considered as a good alternative raw material due to the co-friendly and renewable nature [4]. Composite of metal oxide coated with natural cellulose offer various advantages such as low energy-consumption, low density, biodegradable, low-cost materials and available in large quantity.

Indonesia is one of the largest banana producers in the world and experiencing a fast development in increasing production. The production of banana is a continuously increasing annually, which is followed by the producing of large quantity of solid wastes such as empty fruit bunch. Biochemical and ultimate

analysis proved that banana fruit bunch consists of cellulose (8.8%), hemicellulose (21.23%), lignin (19.06%) and carbon (41.75%), hydrogen (5.10%), oxygen (51.73%), nitrogen (1.23%) [5]. These data revealed that banana fruit bunch is a good alternative as the raw material for production of cellulose and is interesting to explore as an adsorbent for removal or recovery of dyes from wastewater [6,7,8].

Recently, utilizations of by-product with high cellulose have a great progress in research and its application as an adsorbent for developing sustainable and environmentally friendly resources [9,10]. However, natural cellulose has some weaknesses as adsorbent such as the unpredictable mechanism and barrier properties. The improvement of the performance of an adsorbent prepared from the natural cellulose can be achieved by the modification process using metal oxide. The natural cellulose is a polymeric composite which can be explored as matrixes to provide the particular the tensile strength, flexural strength and elongation at breaks. Combinations with suitable ratio of natural cellulose and metal oxide have been intensively studied to form the composite metal oxide/ cellulose and used as an adsorbent for removal of dyes [11,12].

The aim of the present work is to obtain the features of nanomaterial composite of TiO<sub>2</sub>/ cellulose from banana fruit bunch. The characterization of TiO<sub>2</sub>/ cellulose was carried out by SEM, XRD, FTIR and SAA. The effectiveness of composite was investigated for removal of rhodamine B from aqueous solution at different adsorption parameters involving solution pH, concentration, contact time and adsorbent dose. Experimental adsorptions were carried out by batch methods at room temperature. Adsorption equilibria were investigated by the kinetics adsorption models.

## Materials and Methods

### Material

Banana fruit bunch was collected from the banana seller in Yogyakarta, Indonesia. The chemicals such as rhodamine B, potassium hydroxide (KOH), hydrochloric acid (HCl), nitric acid (HNO<sub>3</sub>) and ethanol were obtained in analytical grade from Merck and used without further purification.

### Preparation of Natural Cellulose

Natural cellulose was prepared from banana fruit bunch waste using carbonization process under steam and chemical activation. The raw material was initially cut in to small pieces in the range of 0.5-1.0 cm, washed with distilled water and then dried in an oven at 110°C for 24 h. The dried sample was soaked in 20% KOH solution and refluxed at 85°C for 6 h. It was washed with distilled water and neutralized with 2 M nitric acid solution to pH 6-7. The sample was carbonized under the steam at 250°C for 5 h and continued to dry in an oven at 110°C for 24 h. Resulted natural cellulose was stored for further analysis.

### Preparation of TiO<sub>2</sub>/Cellulose

The natural cellulose was weighted 100 g and added with 20 g of commercial nanomaterial of TiO<sub>2</sub> in a beaker glass. The mixture was immersed in solution of de-ionized water and ethanol with ratio 1:1 while vigorously stirred for 1 h to homogeneous solution. It was transferred in a hydrothermal reactor, and then nitrogen gas was flowed in to reactor. The reactor was placed into graphite furnace and slowly heated up to 200°C for 4 h. After cooling down, the resulted TiO<sub>2</sub>/cellulose was stored in desiccator for further analysis.

### Adsorption Study

Rhodamine B is a basic dye consisting of heterocyclic aromatic chemical moiety. The stock solution of 1000 ppm dye was quantitatively prepared by dissolving 1 g of rhodamine B in 1000 ml of distilled water. The experimental adsorptions were conducted with different parameters involving solution pH (2, 4, 7 and 10), contact time (15, 30, 45 and 60 min), concentration (5, 10, 15 and 20 ppm) and dosage of adsorbent (0.5, 1.0, 1.5 and 2.0 g). The amount of adsorption was determined by UV-Visible spectrophotometer at 555 nm.

### Characterization of TiO<sub>2</sub>/Cellulose

Characterizations of the cellulose and composite TiO<sub>2</sub>/cellulose were conducted to observe their physical and chemical properties. Surface morphology was determined by the Scanning electron micrograph (SEM). The crystallite phase and crystallographic structure were investigated by the X-Ray

diffraction (XRD). Surface functional groups were studied by the Fourier transform infrared (FTIR) using potassium bromide (KBr) to perform the thin pellet.

### Batch Adsorption Study

The effectiveness of TiO<sub>2</sub>/cellulose was evaluated on the removal of rhodamine B using batch method at room temperature. The adsorption capacity was affected by the various pH solutions, initial concentration, composite dosage and contact time. The concentration of the dye was analyzed using a UV-Vis spectrophotometer at 555 nm. The adsorption capacity by a unit mass of the adsorption percentage (% *R*) and the amount of the equilibrium adsorption, *q<sub>e</sub>* (mg/g) were measured using the following the equation (1) and (2), respectively.

$$\% R = \frac{C_0 - C_t}{C_0} \times 100 \quad (1)$$

$$q_e = \frac{C_0 - C_e}{m} \times V \quad (2)$$

where *C<sub>0</sub>* (mg/L) is the initial concentration; *C<sub>e</sub>* (mg/L) is the concentration absorbed at equilibrium; *C<sub>t</sub>* (mg/L) is the concentration at any time; *m* (g) is the mass of composite and *V* is the volume.

## Results and Discussion

### Collecting, Processing and Characterization of Loaded Cellulose

Photographic pictures of the banana fruit bunch, cellulose and TiO<sub>2</sub>/cellulose were shown in Figure 1. Figure 1(a) shows the raw material from banana Kepok (*Musa paradisiaca* L.) from Yogyakarta Indonesia. Figure 1(b) and 1(c) are natural cellulose from banana Kepok and TiO<sub>2</sub>/cellulose composite, respectively. The brown color of cellulose was modified with nitric acid to remove the lignin and other impurities in the cellulose. The addition of nanomaterial of TiO<sub>2</sub> to the celluloses was successfully changed the color from dark brow to grey as a result of loaded TiO<sub>2</sub> to the cellulose materials.



**Figure 1:** Photographic pictures: (a) banana fruit bunch; (b) natural cellulose; (c) TiO<sub>2</sub>/ cellulose

### Determination of Surface Morphology

Overviews of surface morphology for the cellulose and TiO<sub>2</sub>/cellulose composite are shown in Figure 2. An alkaline and acidic treatments with potassium hydroxide and nitric acid played important rule for the acceleration of the removal of lignin, hemicellulose and other impurities attached on the surface of the cellulose including the formation of pores and functional groups [13]. The smooth surface with a cross-section structure is clearly shown as natural cellulose as displayed in Figure 2(a). The surface morphology of the cellulose was clearly observed with an irregular form due to the chemical activation process [14]. The attachment of TiO<sub>2</sub> on the cellulose was confirmed by the SEM as shown in Figure 2(b). The surface morphology of TiO<sub>2</sub>/cellulose was clearly observed as an increase with the roughness of the surface with a cross-sectional irregular form. This result showed that the surface was partially loaded by the TiO<sub>2</sub> as a coating process of TiO<sub>2</sub>/cellulose.

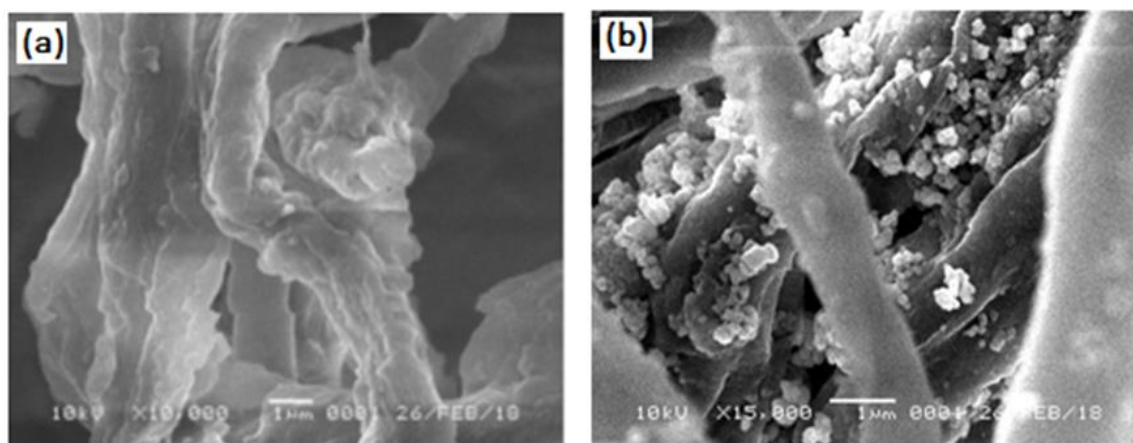


**Figure 2:** Scanning electron micrographs: (a) natural cellulose materials; (b) TiO<sub>2</sub>/cellulose

### Determination of Functional Groups of the Cellulose

Infrared spectroscopy gives one of the useful information for investigating the structure and functional groups. The FTIR spectra of the cellulose and TiO<sub>2</sub>/cellulose are obtained from the wave number in the range of 4000-400 cm<sup>-1</sup> as shown in Figure 3. The FTIR spectra for the cellulose and TiO<sub>2</sub>/cellulose are shown in Figure 3(a) and Figure 3(b), respectively. The strong bands at 3336 and 3334 cm<sup>-1</sup> are assigned to strong hydrogen-bonded OH stretching. The intensity of the TiO<sub>2</sub>/cellulose band shows lower than that of the cellulose due to the replacement of O-H to TiO<sub>2</sub> bond. The formation of crystalline index of the TiO<sub>2</sub>/cellulose proved that there was a degraded amorphous structure of cellulose by reducing amount of hydrogen bonding and replacing with Ti-O bonds. The strong bands found at around 2906 and 2896 cm<sup>-1</sup> are attributed to the symmetrical stretching of aliphatic C-H groups. The bands around 1633 and 1591 cm<sup>-1</sup> are related to OH stretching vibration of adsorbed water [15]. The peak at 1315 cm<sup>-1</sup> related to C=O and C-O of the carboxylic groups. The band at around 1159 and 1160 cm<sup>-1</sup> are assigned to the symmetrical stretching of C-O-C groups. The bands found at 1032-1056 cm<sup>-1</sup> are assigned to C-C, C-OH and C-H ring and side group vibration. The presences of C-O-C, C-C-O and C-C-H deformation and stretching on the cellulose are attributed to band 896 cm<sup>-1</sup> the; C-OH out-of-plane at band 550 cm<sup>-1</sup>. The presence of additional peak at band 450 cm<sup>-1</sup> on the TiO<sub>2</sub>/cellulose spectra is assigned to the Ti-O bond. Based on the FTIR spectra, it can be concluded that TiO<sub>2</sub>/cellulose contains oxygen functional groups.

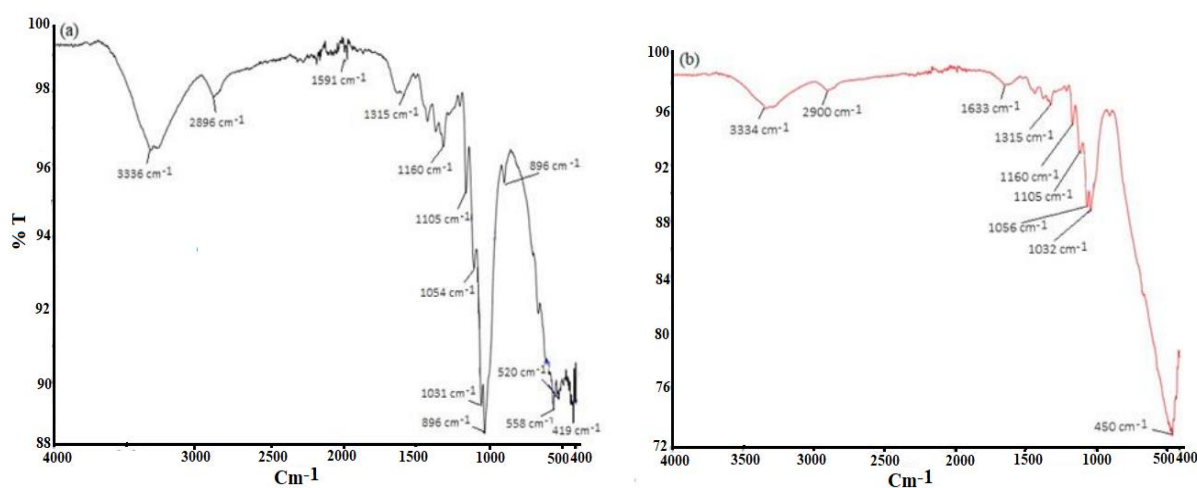


**Figure 3:** FTIR spectra (a) natural cellulose and (b) TiO<sub>2</sub>/cellulose

### Determination of XRD

The X-ray diffraction patterns of the cellulose and nanomaterial of TiO<sub>2</sub>/cellulose were investigated for studying the molecular structure and crystalline phase as shown in Figure 4. The data was taken for the

$2\theta$  ranging from  $10^\circ$  to  $85^\circ$ . Figure 4(a) shows the activated carbon pattern that exhibits the diffraction patterns with two broad diffraction peaks at around  $2\theta = 15.8^\circ$  and  $23.2^\circ$  indicating predominantly amorphous structures. Figure 4(b) is the diffraction patterns of  $\text{TiO}_2/\text{cellulose}$  composite (based on the high-intensity crystal peaks) located at around  $2\theta = 25.8^\circ, 38.3^\circ, 48.5^\circ, 54.3^\circ, 55.5^\circ, 63.0^\circ$  and  $75.5^\circ$  that are indexed as (101), (004), (200), (105), (211), (204) and (215), respectively. These results clearly show anatase crystalline phase of  $\text{TiO}_2$  which was confirmed with the JCPDS card no 21-1272 [16, 17, 18].

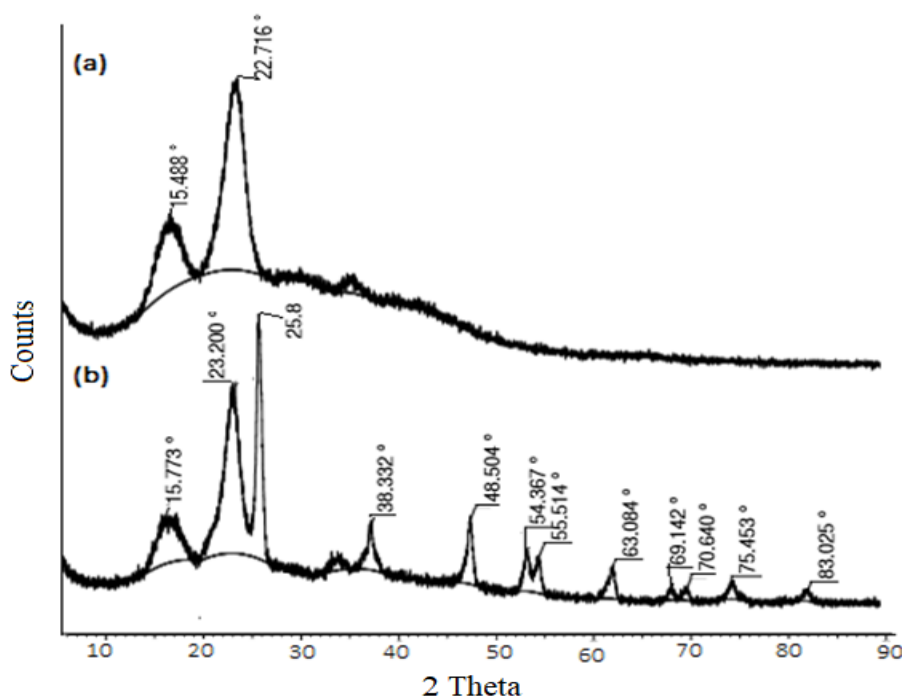


**Figure 4:** X-ray diffraction patterns: (a) cellulose; (b)  $\text{TiO}_2/\text{cellulose}$

### The Effect of pH

Figure 5 showed the effect of rhodamine B adsorption onto  $\text{TiO}_2/\text{cellulose}$  at different pH, contact time, adsorption dosage and concentration. Previous studies reported that the initial pH is an important factor for controlling the adsorption process by the formation of complexation. The effect of pH solution initiated to the change of the charge on composite surface with the change of pH value. The rates of adsorption are performed at different pH ranging from pH 2 to 10. The effect of pH on the  $\text{TiO}_2/\text{cellulose}$  for the removal of rhodamine B is shown in Figure 5(a). The amount of adsorption increases from pH 2 to 4 and then slightly decreases from pH 4 to pH 10. The maximum sorption is obtained at the pH 4 which was used for all experiments. The increase the plot at  $\text{pH} < 4$  could be caused by the formation of the negative charges on the composite surface and the release of proton. Therefore, the zwitterion form of adsorbate is affected by the presence of proton by competing of ions from  $-\text{N}^+$  and  $-\text{COO}^-$ , consequently, the dye becomes lower aggregation by producing positive charges. The electrostatic interaction between the negative charges from the surface of composite and the positive charges from the adsorbate accelerated the formation of complexation. At  $\text{pH} > 4$ , the zwitterion of rhodamine B may increase the aggregation to form a bigger structure and produce negative charges, and then the ionic rhodamine B repelled the ionic composite. This result showed that the decrease of the plot starting from pH 4 to 6 [19].

### Effect of Contact Times

The effects of the contact time on rhodamine B adsorption are shown in Figure 5(b). The experimental data were obtained from the maximum pH 4, volume of rhodamine B 50 ml, weight of

adsorbent 0.5 g, initial concentration 15 ppm and various contact times in the range of 30-60 min. The adsorption rapidly increases at the initial period of contact time to 30 min which is followed with the maximum adsorption. It is because a strong attractive force occurred between the TiO<sub>2</sub>/cellulose composite and the rhodamine B molecules. At the contact time higher than 30 min, the adsorption of the rhodamine B slightly decreases to 45 min and then increases to the end of reaction of 60 min. There is indicative of a weaker attractive force at 45 min indicating of nearly saturated condition. As result, the rhodamine B molecules were adsorbed by the adsorbent and leaved the aqueous solution. The extensions of the contact time have increased the interaction between the rhodamine B molecules and the TiO<sub>2</sub>/cellulose composite followed by an increasing the removal of rhodamine B.

### Effect of Adsorbent Dosage

The effects of the adsorbent dosage on the adsorption of rhodamine B onto TiO<sub>2</sub>/cellulose are shown in Figure 5(c). Investigation of adsorbent dosage was carried out at maximum pH 4, volume of rhodamine B 50 ml with initial concentration 15 ppm, maximum pH 4, and volume of rhodamine B 50 ml, weight of adsorbent 0.5 and various adsorbent dosages in the range of 0.5–2 g. The results showed that the capacity adsorption increases from the 0.5 to 1.0 g and then gradually decreases to the maximum adsorbent dosage of 2 g. The increase of adsorption of the rhodamine B onto the TiO<sub>2</sub>/cellulose composite may be due to the increase of the number of surface area and the availability more pores of the surface of composite. This reason may support to rapid transportation by strongly attractive force between rhodamine B molecules from aqueous solution and active sites of composite. However, the decrease of adsorption capacity is due to reduce of the equilibrium concentration of rhodamine B in aqueous solution with increasing of the adsorbent dosage.

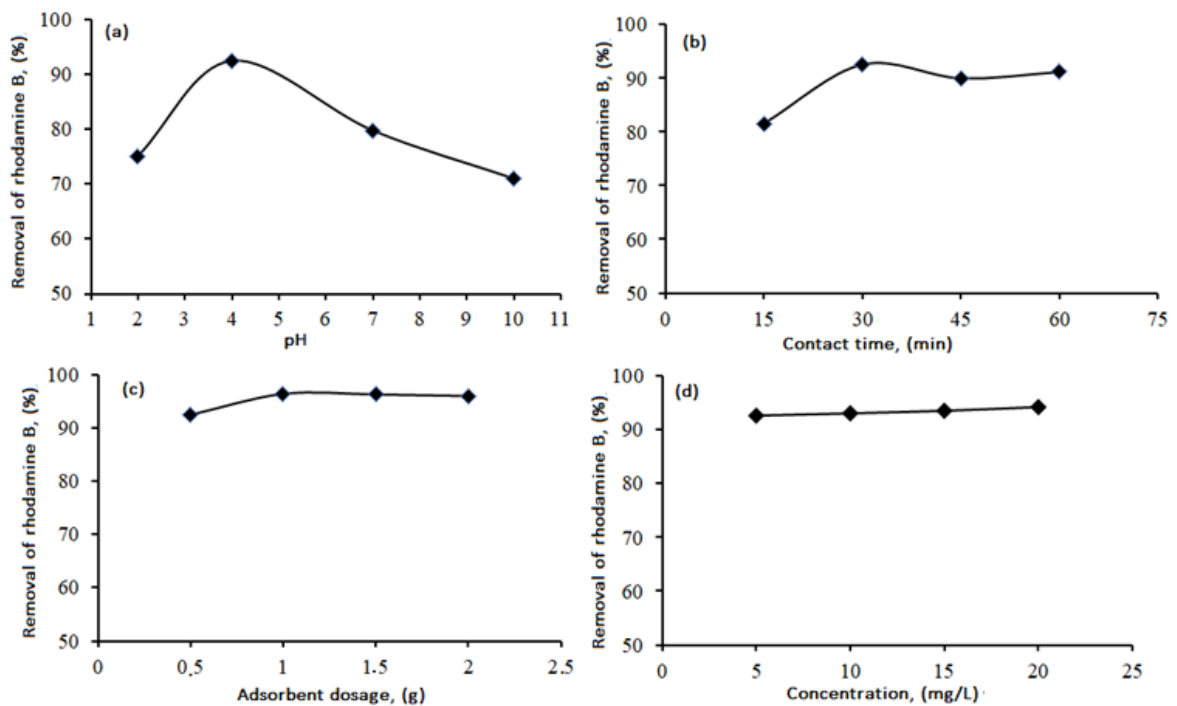


**Figure 5:** Removal of rhodamine B onto TiO<sub>2</sub>/cellulose affected by: (a) pH solution; (b) contact time; (c) adsorbent dosage; (d) concentration

### Effect of Concentration

The effects of the concentration on the adsorption of rhodamine B onto TiO<sub>2</sub>/cellulose composite are illustrated in Figure 5(d). The experiments of the adsorptions are carried out at the different concentrations ranging from 5 to 20 mg/L. At the initial concentration, the percentage of the adsorption increases from 5 to 10 mg/L with the maximum adsorption at 10 mg/L. These features have been noted that with increasing concentration, more rhodamine B molecules can be filled to the vacant pores with the strong attractive force from TiO<sub>2</sub>/cellulose composite. However, at the concentration is higher than 10 mg/L, the percentage adsorption slightly decreased. It assumed due to the saturation of the pores of the adsorbent.

### Adsorption Kinetics

Two models for the kinetics, the pseudo-first-order and pseudo-second-order are used to study the mechanism of rhodamine B removal onto TiO<sub>2</sub>/cellulose.

a. The pseudo-first -order can be expressed as the following eq. 3.

$$\log(q_e - q_t) = \log q_e - \frac{k_1}{2.303} t \quad (3)$$

where  $q_e$  and  $q_t$  are the amounts of rhodamine B adsorbed (mg/g) at the equilibrium and at any time,  $t$  (min), respectively.  $k_1$  (1/min) is rate constant of the adsorption that can be obtained from the plot of  $\ln(q_e - q_t)$  versus  $t$ .

b. The pseudo- second-order can be expressed as the following eq.4.

$$\frac{t}{q_t} = \frac{1}{k_2 q_e^2} + \frac{1}{q_e} t \quad (4)$$

where  $k_2$  is the rate constant (g/mg.min) calculated from the linier plot of  $t$  versus  $t/q_t$  and related with the values of  $q_t$  and the intercept.

Removal of rhodamine B onto TiO<sub>2</sub>/cellulose was evaluated from the plots of pseudo-first-order and second-order as shown in Figure 6. Figure 6(a) and (b) show the plot of pseudo-first and second-order having correlation coefficient close to 1. The kinetic data were calculated from the different contact time data using the plots of  $\log(q_e - q_t)$  versus  $t$  and  $t/q_t$  versus  $t$ , for the pseudo-first-order and the pseudo-second-order, respectively.

The calculation of the pseudo-first and second-order for different temperatures were shown in Table 1. The  $k_1$  of the adsorption parameter for the pseudo-first-order shows negative value due to the fact that there is low interaction occurred between rhodamine B and adsorbent on the monolayer as chemisorption bond. However, the pseudo-second-order shows the best parameter adsorption fitted linearity plot of correlation coefficient ( $R^2 > 0.99$ ). As the result of the kinetic studies indicated that the reaction process of rhodamine B onto TiO<sub>2</sub>/cellulose could be more inclined toward the physisorption.

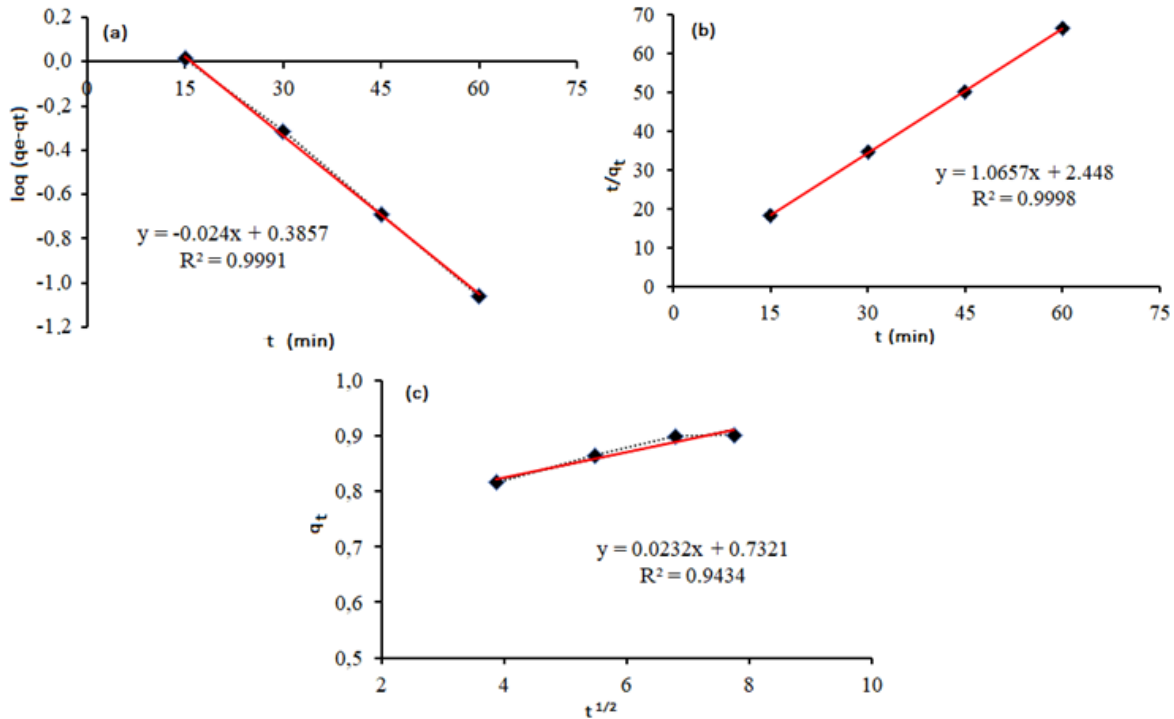


**Figure 6.** Kinetic modeling for adsorption process: (a) pseudo-first-order; (B) pseudo-second-order; (c) and intra-diffusion particle.

**Table 1.** Kinetic Modeling of Removal of Rhodamine B onto TiO<sub>2</sub>/Cellulose.

Pseudo-first-order			Pseudo-second-order			Intra-particle-diffusion		
q <sub>e</sub> (mg/g)	k <sub>1</sub> (1/min)	R <sup>2</sup>	q <sub>t</sub> (mg/g)	k <sub>2</sub> (g/mg.min)	R <sup>2</sup>	K <sub>d</sub> (mg/g min <sup>1/2</sup> )	R <sup>2</sup>	C
2.43	-0.06	0.99	0.94	0.46	0.99	0.02	0.94	0.73

### Intro-particle-diffusion of Rhodamine B

The mechanism of adsorption process can be carried out by several steps involving the transport of adsorbate from aqueous phase to the surface of adsorbent and followed by molecules into the interior of the porous materials [20]. The adsorption process can be described in two ways: (a) the bulk solution transport, the adsorbate diffuse from aqueous solution to the boundary layer surrounding with the adsorbents; (b) the film diffusion: the adsorbate diffuse through the liquid film surrounding with the adsorbents. In this study, the removal of rhodamine B onto porous TiO<sub>2</sub>/cellulose was also controlled by the intra-particle diffusion models that can be expressed as the following eq. 5.

$$q_t = K_d t^{1/2} + C \tag{5}$$

where  $q_t$  (mg/g) is the amount of concentration adsorbed at any time,  $t$  (min),  $K_d$  (mg/g min<sup>1/2</sup>) is the rate constant of the intra-particle diffusion and  $C$  (mg/g) is the intercept representing the thickness of boundary layer; the larger the value of  $C$ , the greater the boundary layer thickness [21]. According to this equation, the curve of  $q_t$  versus  $t^{1/2}$  should be linier, and then the intra-particle diffusion is the rate controlling step. However, if the line is not passing through the origin, it is indicative of the degree of boundary layer control, and the intra-particle diffusion is not the only rate limiting step [22].

Further analysis was carried out from kinetic data for investigating of adsorption mechanism. Intra-particle diffusion of composite was shown in Figure 6(c). It could be suggested that rhodamine B transport onto the composite was controlled by the intra-particle diffusion which was shown by the best linearity of the correlation coefficient ( $R^2 = 9.94$ ). However, the line does not pass through the origin. It proved that the intra-particle diffusing is not rate-controlling step for the adsorption in the system.

## Conclusion

The composite of TiO<sub>2</sub>/cellulose was successfully prepared and characterized. The Scanning electron micrograph (SEM) reveals a strong attractive force between the cellulose and titanium oxide with an increase the roughness on the surface. The X-Ray diffraction (XRD) analysis showed an increasing quality of structure from the amorphous to the anatase crystalline phase. The kinetic adsorption showed a well pseudo-second-order with correlation coefficient ( $R^2 > 0.99$ ) and undesirable popular for the pseudo-first-order. As a result of this study, TiO<sub>2</sub>/cellulose from banana fruit bunch can be used as an adsorbent and required more improvement of their physical and chemical properties.

**Acknowledgments:** The authors gratefully acknowledge the financial support received from the Faculty Mathematic and Natural Sciences and Director of research and public service of Indonesia Islamic University.

**Conflicts of Interest:** The authors declare that there is no conflict of interest in this research

## References

- [1] L. Chen, Y. Lia, S. Hua, J. Suna, Q. Dua, X. Yanga, Q. Jia, Z. Wanga, D. Wanga, Y. Xiaa, Y. Removal of methylene blue from water by cellulose/graphene oxide fibers, *Journal of Experimental Nanoscience*, 11 (2016) 1156-1170.
- [2] S. A. Kosa, N. M. Al-sebaili, I. H. A. El Maksod, E. Z. Hegazy, New method for removal of organic dyes using supported iron oxide as a catalyst, *Journal of Chemistry* (2016) Article ID 1873175.
- [3] D. Suteu, G. Biliuta, L. Rusu, S. Coseri, G. Nacu, Cellulose cellets as new type of adsorbent for the removal of dyes from aqueous media, *Environmental Engineering and Management Journal* 14(2015) 525-532.
- [4] C. S. Ajinomoh, N. Salahudeen, Production of activated carbon from sugar cane bagasse, *Australian Society for Commerce Industry & Engineering* (2014) 16-22.
- [5] P. Sugumaran, P.V. Susan, P. Ravichandran, S. Seshadri, Production and characterization of activated carbon from banana empty fruit bunch and delonix regia fruit pod, *Journal of Sustainable Energy & Environment*, 3(2012) 125-132.
- [6] A. Karim, S.F. Lim, S.N.D. Chua, S.F. Salleh, P.L. Law, Banana fibers as sorbent for removal of acid green dye from water, *Journal of Chemistry* (2016) 11, 1-11.
- [7] M.A. Khaleque, D.K. Roy, Removing reactive dyes from textile effluent using banana fibre, *International Journal of Basic & Applied Sciences* (2016)16, 14-20.
- [8] G. Annadurai, R.S. Juang, D. J. Lee, Adsorption of heavy metals from water using banana and orange peels, *Water Science and Technology* 47(2002) 185-190.
- [9] X. Yue, J. Huang, F. Jiang, H. Lin, Y. Chen, Synthesis and characterization of cellulose-based adsorbent for removal of anionic and cationic dyes, *Journal of Engineered Fibers and Fabrics* 14(2019) 1-10.
- [10] C Fard, M. Mirjalili, F. .Najafi, Preparation of nano-cellulose/A-Fe<sub>2</sub>O<sub>3</sub> hybrid nanofiber for the cationic dyes removal: optimization characterization, kinetic, isotherm and error analysis, *Bulgarian Chemical Communication* 50 (2018) 251-261.
- [11] A. A. Moosa, A.M. Ridha, N. A. Kadhim, Use of bio-composite adsorbents for the removal of methylene blue dye from aqueous solution, *American Journal of Materials Science* 6(2016), 135-146.
- [12] N. Jallouli, K. Elghniji, H. Trabelsi, M. Ksibi, Photocatalytic degradation of paracetamol on TiO<sub>2</sub> nanoparticles and TiO<sub>2</sub>/cellulosic fiber under UV and sunlight irradiation. *Arabian Journal of Chemistry* 10 (2017) S3640–S3645.

- 
- [13] M. Tan, L. Ma, M.S. Ur Rahman, M.A. Ahmed, M. Sajid, X. Xu, Y. Sun, P. Cui, J. Xu, Screening of acidic and alkaline pretreatments for walnut shell and corn stover biorefining using two way heterogeneity evaluation, *Renewable Energy* 132(2019) 950-958.
- [14] S. Mopoung, P. Moonsri, W. Palas, S. Khumpai, Characterization and properties of activated carbon prepared from tamarind seeds by KOH activation for Fe(III) adsorption from aqueous solution. *The Scientific World Journal* (2015) 1–9.
- [15] Y.S. Oh, D. II Yoo, Y. Shin, G. Seo, FTIR analysis of cellulose treated with sodium hydroxide and carbon dioxide, *Carbohydrate Research*, 340(2005) 417-428.
- [16] R. Varshney, S. Bhadauria, M.S. Gaur, Biogenic synthesis of silver nanocubes and nanorods using sundried *Stevia rebaudiana* leaves. *Advance Material Letter*, 1 (2010) 232-237.
- [17] Z. Antic, R. M. Krsmanovic, G. Nikolic, M. M. Cincovic, M. Mitric, S. Polizzi, M. D. Dramicanin, Multisite luminescence of rare earth doped TiO<sub>2</sub> anatase nanoparticles. *Material Chemistry and Physics* 135 (2012) 1064-1069.
- [18] J. Zhang, F. Liu, J. Gao, Y. Chen, X. Hao, Ordered mesoporous TiO<sub>2</sub>/activated carbon for adsorption and photocatalysis of acid red 18 solution, *BioRes.* 12 (2017) 9086-9102.
- [19] Y. Ma, N. Gao, W. Chu, C. Li, Removal of phenol by powdered activated carbon adsorption. *Frontiers of Environmental Science & Engineering*, 7 (2013) 158–165.
- [20] W. Weber, J. Morris, Kinetics of adsorption on carbon from solution, *Journal of the Sanitary Engineering Division*, 89 (1963) 31-60.
- [21] S. K. Singh, T.G. Townsend, D. Macyzk, T. H. Boyer, Equilibrium and intra-particle diffusion of stabilized landfill leachate onto micro- and meso-porous activated carbon, *Water Research*, 46 (2012) 491-499.
- [22] P. Panneerselvam, N. Morad, K. A. Tan, R. Mathiyarasi, Removal of rhodamine b dye using activated carbon prepared from palm kernel shell and coated with iron oxide nanoparticles. *Separation Science and Technology*, 47 (2012) 742–752.